

Deep Memory Update

Łukasz Neumann¹, Łukasz Lepak¹ and Paweł Wawrzyński¹

¹Warsaw University of Technology, Institute of Computer Science, Warsaw, Poland
{lukasz.neumann, lukasz.lepak.dokt, pawel.wawrzynski}@pw.edu.pl

Abstract

Recurrent neural networks are important tools for sequential data processing. However, they are notorious for problems regarding their training. Challenges include capturing complex relations between consecutive states and stability and efficiency of training. In this paper, we introduce a recurrent neural architecture called Deep Memory Update (DMU). It is based on updating the previous memory state with a deep transformation of the lagged state and the network input. The architecture is able to learn to transform its internal state using any nonlinear function. Its training is stable and fast due to relating its learning rate to the size of the module. Even though DMU is based on standard components, experimental results presented here confirm that it can compete with and often outperform state-of-the-art architectures such as Long Short-Term Memory, Gated Recurrent Units, and Recurrent Highway Networks.

1 Introduction

Recurrent Neural Networks (Recurrent NNs, RNNs) are designed to process sequential data and are vital components of systems that perform speech recognition [Graves *et al.*, 2013], machine translation [Wu *et al.*, 2016], handwritten text recognition [Capes *et al.*, 2017], and other tasks [Schmidhuber, 2015].

An intuitively designed RNN is prone to gradient explosions or vanishing [Bengio *et al.*, 1994] due to its recurrent nature. The impact of a given input on future outputs of the RNN may vanish or explode with time. Specialized architectures with gates, namely Long Short-Term Memory (LSTM) networks [Hochreiter and Schmidhuber, 1997] and Gated Recurrent Unit (GRU) networks [Cho *et al.*, 2014a], are designed to overcome this problem at the level of a single neuron. While these networks are widely successful, they come with a cost — their memory state undergoes only single layer transformation from one time instant to another.

Several recurrent architectures apply deep processing of their internal states [Pascanu *et al.*, 2013; Chung *et al.*, 2015; Zilly *et al.*, 2017]. However, they are complex or are challenging to train.

This paper addresses the above shortcomings by introducing a neural module designed to prevent the previously mentioned gradient problems while allowing the state transformation to be modelled by an arbitrary feedforward neural network. We call this module Deep Memory Update (DMU). As a result, state transformation can easily be shaped in DMU. Additionally, the architecture is resistant to problems of gradient exploding/vanishing. Experimental results presented in the paper confirm that DMU performs well in comparison to its state-of-the-art counterparts.

RNNs are often outperformed by feedforward networks with attention, especially by the transformer [Vaswani *et al.*, 2017]. However, the computational complexity of these techniques excludes them from some applications [Jia *et al.*, 2021; Hansen *et al.*, 2020]. It is also reasonable to expect that some combination of attention and RNNs, such as R-Transformer [Wang *et al.*, 2019], ASRNN [Lin *et al.*, 2021] and others [Liu *et al.*, 2020], will outperform both. Therefore, in this paper, we focus solely on RNNs.

2 Related work

Early RNNs [Jordan, 1986; Elman, 1990; Robinson and Fallside, 1987; Werbos, 1988] suffered from the problem of gradient vanishing/exploding defined by Bengio *et al.* [1994]: A small change in the RNN’s weights causes its future output’s change that is vanishing or exploding in time. As a result, the impact of RNN’s weights on its performance is either close to zero or infinity. In either case, it is impossible to train such a network. A gradient norm clipping strategy proposed in [Pascanu *et al.*, 2013] may mitigate this problem to some extent. [Arjovsky *et al.*, 2016] used orthogonal matrices of weights in shallow RNNs to stabilize the gradient successfully.

The gradient vanishing/exploding problem was alleviated at a cell level with Long Short-Term Memory (LSTM) networks [Hochreiter and Schmidhuber, 1997]. A neuron in such a network is a state machine with several so-called gates. The neuron generally preserves its state from one time to another but may also change it. The change depends on the dot product of the neuron inputs and its weights computed in its gates. LSTMs have been enhanced with batch normalization of a recurrent signal [Cooijmans *et al.*, 2017].

Cho *et al.* [2014a] proposed an architecture based on neurons simpler than those in LSTMs, called Gated Recurrent Units (GRUs). Despite its simplicity, it generally preserved

the favourable properties of LSTM. Li *et al.* [2018] proposed a unit whose state was only computed based on its previous state and the outputs of the preceding neural layer. Networks based on such units, Independently Recurrent Neural Networks (IndRNNs), tend to outperform LSTMs and GRUs.

Capturing long-term dependencies in input sequences is a crucial challenge that RNNs face. Chang *et al.* [2017] proposed to increase lag of recurrent connections in higher network layers geometrically. Campos *et al.* [2018] introduced SkipRNN that learns to skip state updates and shorten the effective size of the computational graph. Tallec and Olivier [2018] prove that RNNs operate via transformations of time, and the gates in LSTM and GRU networks are a straightforward way to perform these transformations.

LSTMs and GRUs are usually organized in several layers stacked on top of one another [Graves, 2013]. Input to each neuron within a layer includes the previous states of all the neurons in the layer. This way, at each time instant, the network input undergoes a deep transformation. However, the internal state of the network undergoes only a shallow, single-layer transformation.

Being able to apply an arbitrary nonlinear, deep transformation to its internal state is a valuable feature of a recurrent neural network. Pascanu *et al.* [2014] proposed to increase the recurrence depth by adding multiple nonlinear layers to the recurrent transition, resulting in Deep Transition RNNs (DT-RNNs) and Deep Transition RNNs with Skip connections (DT(S)-RNNs). Gradient propagation issues are exacerbated in these architectures due to long credit assignment paths. Chung *et al.* [2015] added extra connections between all states across consecutive time steps in a stacked RNN, which also increases recurrence depth. However, their model requires additional connections with increasing depth, gives only a fraction of state cells access to the deepest layers, and faces gradient propagation issues along the longest paths.

Zilly *et al.* [2017] introduced Recurrent Highway Networks (RHNs), which can be understood as LSTMs with specialized multilayer gates. These networks apply deep processing to their internal state while successfully coping with gradient vanishing/exploding.

A number of concepts may facilitate the performance of RNNs. Le *et al.* [2015] proposed a scheme of initialization of weights in these networks. RNNs are usually trained with Stochastic Gradient Descent with gradient estimates computed with backpropagation through time. However, recent work of Kag and Saligrama [2021] on forward propagation through time calls this practice into question.

3 Method

In this section, we introduce the Deep Memory Update (DMU) module. It is a neural module with memory designed to have the following properties:

1. Its memory state can undergo an arbitrary nonlinear transformation from one moment to another.
2. The module can easily preserve its memory state from one moment of time to another.
3. Its learning is relatively fast and stable.

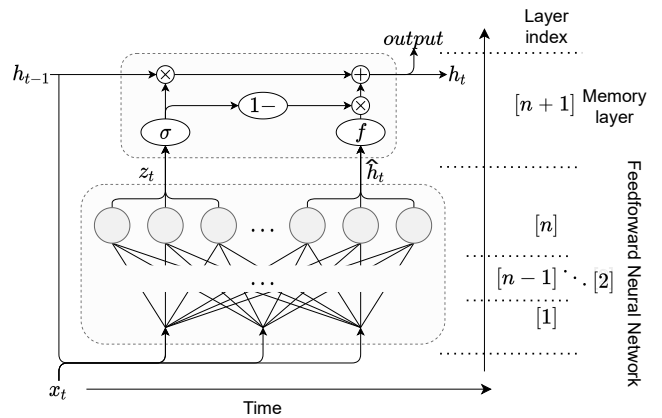


Figure 1: Structure of Deep Memory Update module. The module comprises the feedforward neural network, which can arbitrarily process the state and a memory layer. The output of the module is also its hidden state.

3.1 General structure

We present the structure of the Deep Memory Update (DMU) module in Fig. 1. The module operates in discrete time $t = 1, 2, \dots$. At each time, the module is fed with the input $x_t \in \mathbb{R}^m$ and produces the vector $h_t \in \mathbb{R}^d$ which is both its memory state and its output.

A lagged memory state, h_{t-1} , together with an input of the block, x_t , are fed to a feedforward neural network, FNN. The network’s output layer is linear with $2d$ neurons. It produces two vectors: $z_t \in \mathbb{R}^d$ determines to what extent the memory state should be preserved, and $\hat{h}_t \in \mathbb{R}^d$ determines the direction in which the state should change.

A pair of i -th elements of z_t and \hat{h}_t are fed to a i -th memory cell. The new cell state is a weighted, with z_t , average of the old state, h_{t-1} , and \hat{h}_t . The memory state update takes the form

$$\langle z_t, \hat{h}_t \rangle = \text{FNN}(h_{t-1}, x_t) \quad (1)$$

$$h_t = h_{t-1} \circ \sigma(z_t) + f(\hat{h}_t) \circ (\mathbf{1} - \sigma(z_t)), \quad (2)$$

where “ \circ ” denotes the elementwise product, $\mathbf{1}$ is a vector of ones, σ is a unipolar soft step function, e.g. the logistic sigmoid,

$$\sigma_i(z) = \frac{e^{z_i}}{1 + e^{z_i}} \text{ for } z_i \in \mathbb{R},$$

and f is an activation function, e.g.

$$f_i(z) = \tanh(z_i) \text{ for } z_i \in \mathbb{R}.$$

Our proposed recurrent architecture is compared with GRU [Cho *et al.*, 2014a] in the supplementary material.

Let us consider how the required properties of DMU are achieved.

1. Since a feedforward neural network with at least two dense layers is a universal function approximator, the network state can undergo the arbitrary nonlinear transformation from one time moment to another.
2. The block preserves its memory state for large values of z_t . In particular, for $z_t = +\infty$ we have $h_t = h_{t-1}$.

3. For efficient and stable training of the network, it is enough that the learning rate of the module is sufficiently lower than that of the rest of the network, as discussed in Section 3.3.

3.2 Initialization

The FNN block should be a universal approximator. It can be a multilayer perceptron with at least two layers, including a linear output layer. This layer needs to be linear because its output should not be limited. It should be possible that $z_t \gg 1$ which causes the memory state to be preserved, $h_t \cong h_{t-1}$.

We recommend using the standard ways of initializing neural weights in the FNN block, with one exception. Namely, upon weights’ initialization, we recommend adding a positive scalar to the biases of the neurons that produce z_t values, e.g., 3. With positive elements of z_t , the memory state of the DMU module will be, by default, largely preserved from one moment t to another.

3.3 Training

Training of DMU may be based on gradient backpropagation through time and using the gradient with a method of stochastic optimization such as Stochastic Gradient Descent or ADAM [Kingma and Ba, 2014]. These methods apply a learning rate to each trained weight. In turn, the learning rate defines a speed of optimization along derivatives with respect to this weight. Typically, the learning rates are equal for all weights.

Let us consider DMU as a module in a feedforward architecture. Its learning speed and stability can be noticeably improved by distinguishing a module’s learning rate and setting its value smaller than that of the rest of the architecture. The learning of recurrent modules is exposed to instability, which naturally limits its learning speed. Nevertheless, it does not need to limit the learning speed of the surrounding feedforward modules, which are less exposed to instability, thus may learn faster.

In our experiments in Sec. 4 we combine n -layer DMU modules with n' -layer feedforward output subnetworks. For $\beta > 0$ being a learning rate for the output subnetwork we use a learning rate of the DMU module, β_{DMU} , equal to

$$\beta_{\text{DMU}} = \frac{\beta}{2n}. \quad (3)$$

The deeper the DMU module, the smaller its learning rate. Additionally, when weight decay is used in the network training, its strength in the DMU module is reduced $2n$ times.

3.4 Gradient vanishing and exploding

The gates in LSTM, GRU and RHN play the following role: The state of the network is generally preserved, and the gradient flows back through the time at a similar magnitude. The gates learn to identify parts of the state that need to be incrementally changed according to the current input and state. DMU does not introduce any novelty in this particular mechanism because it is also based on gates. The parts of the state that need an increment and the increment alone can be identified accurately due to the DMU’s gates, which can generally represent any nonlinear transformation.

4 Experimental study

To evaluate the DMU architecture, we test it on three synthetic problems and three modern problems based on real-life data. The synthetic problems are taken from [Hochreiter and Schmidhuber, 1997], and are noisy sequences, adding, and temporal order. The modern data-based problems are polyphonic music modelling [Boulanger-Lewandowski *et al.*, 2012], natural language modelling [Zaremba *et al.*, 2014], and Spanish/German/Portuguese to English machine translation tasks [Tatoeba, 2020; ManyThings, 2020].

We compare our DMU module using shallow architectures with ordinary recurrent neural networks (RNNs), GRU, LSTM, and RHN in the synthetic problems. We also compare DMU in its deep version with RHN in the data-based problems. To make the comparison fair, we embed a recursive subnetwork within the same neural architecture. That subnetwork is a layer or a few layers of recurrent units or a DMU module or RHN. Moreover, for each depth of RNNs, we compare different architectures of similar sizes measured by the number of weights.

A reader may find details of our experimental setting, hyperparameters of architectures and their training in the supplementary material.

4.1 Adding problem

The first task will be called “Adding”. It is taken from [Hochreiter and Schmidhuber, 1997, sec. 5.4].

Results. We present the results for the adding problem in Fig. 2. We conclude that DMU significantly outperforms all other modules, and GRU scores better than LSTM. RNN and RHN are not able to reach any threshold within 100 training epochs for any hyperparameters.

4.2 Temporal order

The next task, referred to as “TempOrd” is taken from [Hochreiter and Schmidhuber, 1997, sec. 5.6, Task 6b].

Results. The results for the TempOrd task are depicted in Fig. 3. We note that DMU has faster convergence than GRU and maintains similar results for high thresholds (up to 10^{-4}). For lower thresholds, DMU outperforms GRU. LSTM reaches partial success on higher thresholds but fails for lower ones. RNN and RHN fail for all thresholds without a single successful 100 epoch run.

4.3 Noise-free and noisy sequences

We call this task “NoiseSeq”. It is taken from [Hochreiter and Schmidhuber, 1997, sec. 5.2].

Results. Figure 4 contains the results for the NoiseSeq task. We observe that GRU and DMU obtain similar results, in most cases reaching all the loss thresholds, with GRU training faster. RHN in about half of the cases does not reach any threshold, and in the other half, it reaches all of them. RNN performs worse than RHN, and LSTM performs worse than RNN.

4.4 Polyphonic music modelling

In this subsection, we evaluate modules on the polyphonic music modelling task, referred to as “PolyMusic”, based on

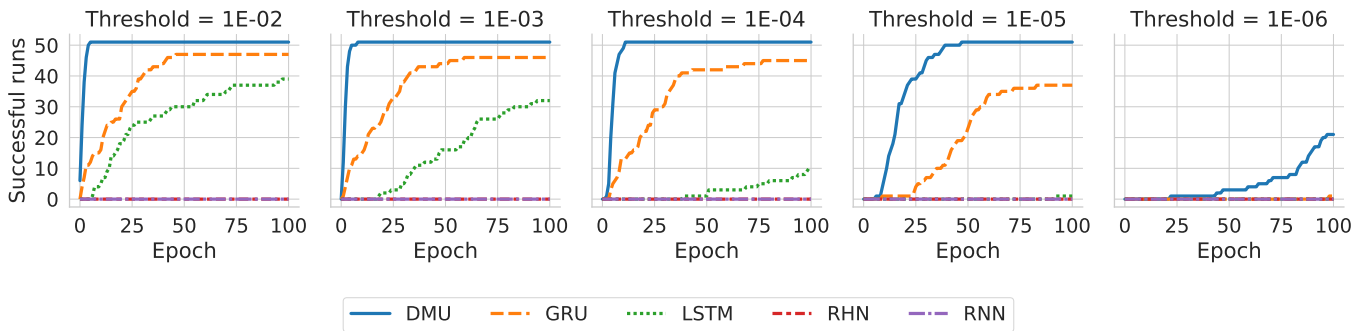


Figure 2: Adding: Results of 51 runs, five graphs for different loss thresholds, a curve presents how many runs reach a given loss threshold at a given training epoch.

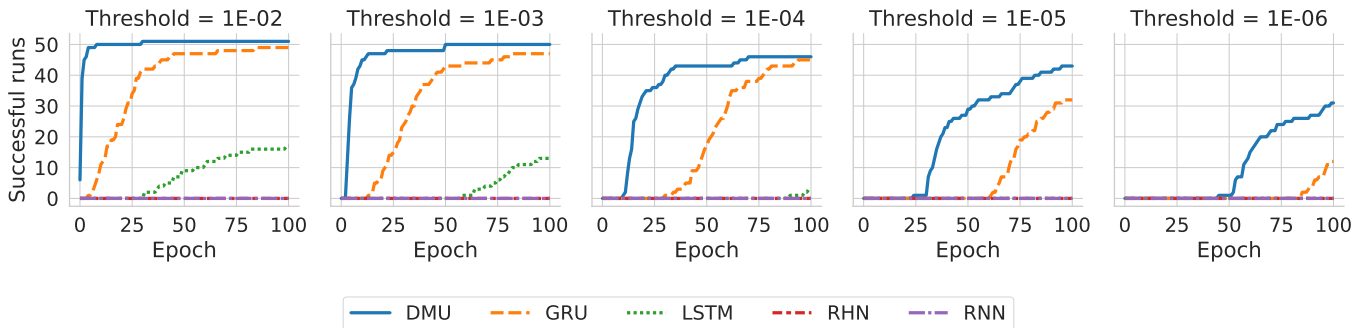


Figure 3: TempOrd: Results of 51 runs, five graphs for different loss thresholds.

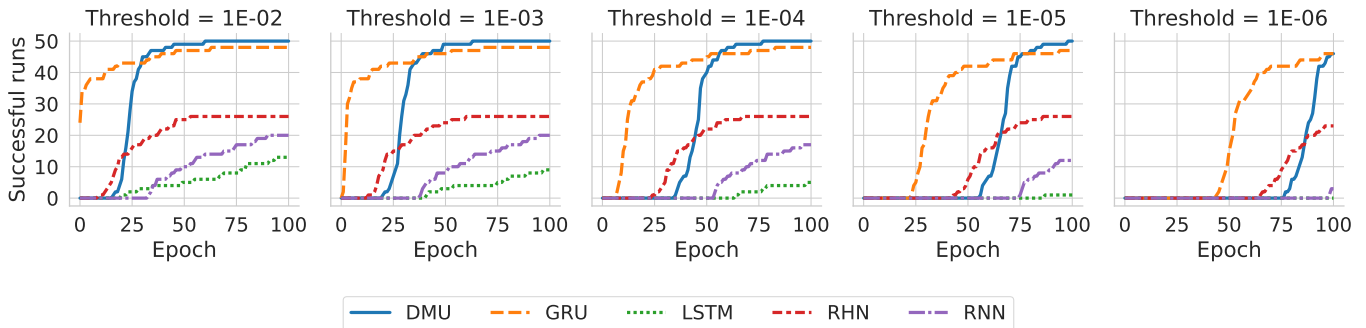


Figure 4: NoiseSeq: Results of 51 runs, five graphs for different loss thresholds.

the Nottingham music dataset [Boulanger-Lewandowski *et al.*, 2012].

Results. The results of the polyphonic music modelling can be found in Table 1. In this problem, DMU outperforms RHN at 3 out of 4 depths with regard to test mean loss.

4.5 Natural language modelling

The task called “NatLang” is based on the Penn Treebank corpus of English [Marcus *et al.*, 1993].

Results. Table 2 shows the results. DMU achieves consistently better results than RHN, often by a large margin. Only for a depth of 2 RHN performs slightly better than DMU with respect to the mean test perplexity.

4.6 Machine translation

Finally, we test the modules in the context of machine translation, using recurrent architectures. The task is based on datasets of pairs of corresponding Spanish/Portuguese/German and English sentences [Tatoeba, 2020; ManyThings, 2020]. We will call experiments based on subsequent pairs “Spa2Eng”, “Por2Eng”, and “Ger2Eng”.

Results. Table 3 contains the results. DMU achieves better accuracy than RHN for all three language pairs at each depth of both networks. Additionally, both networks score the best accuracy for a depth of 1 or 2. Accuracy generally deteriorates with growing depth, significantly faster for RHN than for DMU.

depth	model	train			test		
		best	mean	std dev.	best	mean	std dev.
1	RHN	3.344	3.375	0.078	3.552	3.598	0.037
	DMU	2.942	2.959	0.042	3.567	3.631	0.050
2	RHN	3.390	3.414	0.098	3.553	3.607	0.063
	DMU	3.022	3.094	0.067	3.487	3.551	0.041
5	RHN	3.443	3.682	0.163	3.734	3.851	0.106
	DMU	3.215	3.208	0.064	3.630	3.685	0.032
10	RHN	3.701	3.927	0.143	3.903	4.075	0.118
	DMU	3.523	3.537	0.149	3.951	4.044	0.087

Table 1: PolyMusic: results — loss

depth	model	train			test		
		best	mean	std dev.	best	mean	std dev.
1	RHN	61.102	66.531	6.071	106.105	110.394	4.363
	DMU	56.625	59.422	3.137	105.354	106.129	0.475
2	RHN	62.895	66.317	4.232	104.888	109.833	4.040
	DMU	64.421	64.861	1.434	109.601	110.128	0.465
5	RHN	82.325	86.097	3.832	123.158	124.971	1.923
	DMU	92.395	94.063	1.114	117.924	120.368	1.456
10	RHN	85.972	149.430	86.869	124.458	171.598	60.383
	DMU	118.199	119.475	1.526	130.054	131.827	1.440

Table 2: NatLang: results — perplexity

lang pair	depth	model	train			test			
			best	mean	std dev.	best	mean	std dev.	
Spa2Eng	1	RHN	0.893	0.909	0.012	0.688	0.684	0.003	
		DMU	0.930	0.927	0.003	0.697	0.692	0.005	
	2	RHN	0.911	0.908	0.011	0.686	0.680	0.003	
		DMU	0.938	0.937	0.009	0.691	0.686	0.005	
	5	RHN	0.761	0.680	0.059	0.574	0.549	0.021	
		DMU	0.837	0.829	0.007	0.661	0.653	0.005	
	10	RHN	0.304	0.275	0.017	0.306	0.283	0.012	
		DMU	0.760	0.749	0.009	0.629	0.625	0.003	
	Por2Eng	1	RHN	0.937	0.935	0.006	0.776	0.768	0.005
			DMU	0.926	0.941	0.008	0.776	0.773	0.003
2		RHN	0.928	0.932	0.008	0.769	0.761	0.005	
		DMU	0.955	0.952	0.006	0.775	0.768	0.004	
5		RHN	0.899	0.834	0.103	0.720	0.674	0.054	
		DMU	0.861	0.861	0.004	0.731	0.725	0.005	
10		RHN	0.396	0.312	0.042	0.380	0.310	0.035	
		DMU	0.807	0.803	0.012	0.709	0.706	0.003	
Ger2Eng		1	RHN	0.915	0.920	0.008	0.746	0.744	0.001
			DMU	0.924	0.925	0.006	0.753	0.749	0.003
	2	RHN	0.921	0.924	0.006	0.741	0.736	0.005	
		DMU	0.935	0.938	0.005	0.749	0.743	0.004	
	5	RHN	0.830	0.775	0.044	0.670	0.635	0.022	
		DMU	0.845	0.843	0.010	0.711	0.703	0.006	
	10	RHN	0.442	0.350	0.064	0.448	0.348	0.063	
		DMU	0.797	0.782	0.011	0.684	0.679	0.004	

Table 3: Translation: results — accuracy

4.7 Learning rate ablation

We verify how a reduction of a DMU learning rate according to (3) impacts the performance of the neural architecture with this module. In this order, we register the performance of each architecture with approximately optimized, with a grid search,

learning rate. In one variant, the learning rate is constant for the whole architecture. In the other, the learning rate of the DMU module and the learning rate for the rest are bound with (3). The results confirm that efficiency benefits from reducing the learning rate of the DMU module. Numeric results are presented in the supplementary material.

5 Discussion

Since the seminal paper of Hochreiter and Schmidhuber [1997] the development of recurrent neural networks has been stimulated by the need to avoid gradient exploding or vanishing in backpropagation through time. Indeed, these phenomena are likely to occur in neural networks with feedback loops. In LSTM and GRU architectures, they were eliminated at the cell level.

The DMU neural module introduced in this paper is based on memory cells whose state is updated with the weighted average of their previous content and new values proposed for them. Both the weights and the new proposed values come from a feedforward subnetwork whose inputs include the previous state of the memory cells. Architectures based on the DMU module compete with and often outperform those based on LSTM or GRU. The gradient vanishing/exploding problem is solved in DMU at the module level.

In some applications, deep transformation of the network state is necessary. However, then the effective length of the gradient path increases, which may destabilize training. RHN successfully coped with this problem at the expense of the complexity of its architecture. DMU applies a typical feedforward block of any depth for state transformation. Training stability is ensured by appropriately reducing the learning rate of the DMU module. As a result, DMU performed better than RHN of the same depth in all three analyzed data-based problems with a handful of exceptions.

Interestingly, contrary to Zilly *et al.* [2017] we note that depth-scaling of the model did not yield better results. We speculate that it can be explained by the lack of regularization other than weight decay. This was a deliberate choice to compare RHN and DMU modules without any unnecessary architectural additions.

6 Conclusions

In this paper, we propose DMU — a recurrent neural module that can perform an arbitrary nonlinear transformation of its memory state. Three experiments with synthetic data (Adding, Temporal order, Noisy sequence) presented here compare neural architectures based on DMU with those based on RNN, LSTM, and GRU. Three experiments with real-life data (Polyphonic music, Natural language modelling, Machine translation) compare neural architectures based on DMU with those based on Recurrent Highway Networks of the same depth. The architecture based on DMU outperformed RHN in 18 out of 20 analyzed mean test score cases.

Acknowledgments

We gratefully acknowledge the contribution of Aleksander Zamojski, Lidia Wojciechowska and Monika Berlińska to the code of DMU.

References

[Arjovsky *et al.*, 2016] M. Arjovsky, A. Shah, and Y. Bengio. Unitary evolution recurrent neural networks. In *ICML*, pages 1120–1128, 2016.

[Bengio *et al.*, 1994] Y. Bengio, P. Simard, and P. Frasconi. Learning long-term dependencies with gradient descent is difficult. *IEEE Transactions on Neural Networks*, 5(2):157–166, 1994.

[Boulanger-Lewandowski *et al.*, 2012] N. Boulanger-Lewandowski, Y. Bengio, and P. Vincent. Modeling temporal dependencies in high-dimensional sequences: Application to polyphonic music generation and transcription. In *ICML*, 2012.

[Campos *et al.*, 2018] V. Campos, B. Jou, X. Giro i Nieto, J. Torres, and S.-F. Chang. Skip rnn: Learning to skip state updates in recurrent neural networks. In *ICLR*, 2018.

[Capes *et al.*, 2017] T. Capes, P. Coles, A. Conkie, L. Golipour, A. Hadjitarkhani, Q. Hu, N. Huddleston, M. Hunt, J. Li, M. Neeracher, and K. Prahallad. Siri on-device deep learning-guided unit selection text-to-speech system. In *Interspeech*, pages 4011–4015, 2017.

[Chang *et al.*, 2017] S. Chang, Y. Zhang, W. Han, M. Yu, X. Guo, W. Tan, X. Cui, M. Witbrock, M. Hasegawa-Johnson, and T. S. Huang. Dilated recurrent neural networks. In *NIPS*, 2017.

[Cho *et al.*, 2014a] K. Cho, B. Van Merriënboer, C. Gulcehre, D. Bahdanau, F. Bougares, H. Schwenk, and Y. Bengio. Learning phrase representations using rnn encoder-decoder for statistical machine translation. In *EMNLP*, 2014.

[Cho *et al.*, 2014b] K. Cho, B. van Merriënboer, D. Bahdanau, and Y. Bengio. On the properties of neural machine translation: Encoder-decoder approaches, 2014. arXiv:1409.1259.

[Chung *et al.*, 2015] J. Chung, C. Gulcehre, K. Cho, and Y. Bengio. Gated feedback recurrent neural networks. In *ICML*, pages 2067–2075, 2015.

[Cooijmans *et al.*, 2017] Tim Cooijmans, Nicolas Ballas, César Laurent, Çağlar Gülçehre, and Aaron Courville. Recurrent batch normalization. In *ICLR*, 2017.

[Elman, 1990] J. L. Elman. Finding structure in time. *Cognitive science*, 14(2):179–211, 1990.

[Graves *et al.*, 2013] A. Graves, A. Mohamed, and G. Hinton. Speech recognition with deep recurrent neural networks, 2013. arXiv:1303.5778.

[Graves, 2013] A. Graves. Generating sequences with recurrent neural networks, 2013. arXiv:1308.0850.

[Hansen *et al.*, 2020] C. Hansen, C. Hansen, L. Maystre, R. Mehrotra, B. Brost, F. Tomasi, and M. Lalmas. Contextual and sequential user embeddings for large-scale music recommendation. In *ACM Conf. on Recommender Systems*, pages 53–62, 2020.

[Hochreiter and Schmidhuber, 1997] S. Hochreiter and J. Schmidhuber. Long short-term memory. *Neural Computation*, 9(8):1735–1780, 1997.

[Jia *et al.*, 2021] Z. Jia, Y. Lin, J. Wang, Z. Feng, X. Xie, and C. Chen. Hetemotionnet: Two-stream heterogeneous graph recurrent neural network for multi-modal emotion

- recognition. In *ACM Int. Conf. on Multimedia*, pages 1047–1056, 2021.
- [Jordan, 1986] M. I. Jordan. Serial order: A parallel, distributed processing approach. *Advances in Connectionist Theory Speech*, 121(ICS-8604):471–495, 1986.
- [Kag and Saligrama, 2021] A. Kag and V. Saligrama. Training recurrent neural networks via forward propagation through time. In *ICML*, pages 5189–5200, 2021.
- [Kingma and Ba, 2014] D. Kingma and J. Ba. Adam: A method for stochastic optimization. In *ICLR*, 2014.
- [Le et al., 2015] Q. V. Le, N. Jaitly, and G. E. Hinton. A simple way to initialize recurrent networks of rectified linear units, 2015. arXiv:1504.00941.
- [Li et al., 2018] S. Li, W. Li, C. Cook, C. Zhu, and Y. Gao. Independently recurrent neural network (indrnn): Building a longer and deeper rnn. In *CVPR*, 2018.
- [Lin et al., 2021] J. C.-W. Lin, Y. Shao, Y. Djenouri, and U. Yun. Asrnn: A recurrent neural network with an attention model for sequence labeling. *Knowledge-Based Systems*, 212:106548, 2021.
- [Liu et al., 2020] Zhenyu Liu, Chaohong Lu, Haiwei Huang, Shengfei Lyu, and Zhenchao Tao. Hierarchical multi-granularity attention-based hybrid neural network for text classification. *IEEE Access*, 8:149362–149371, 2020.
- [ManyThings, 2020] ManyThings. <http://www.manythings.org/anki/>, 2020. Retrieved 2020-05-05.
- [Marcus et al., 1993] M. Marcus, B. Santorini, and M. A. Marcinkiewicz. Building a large annotated corpus of english: The penn treebank. *Computational Linguistics*, 19(2):313–330, 1993.
- [Pascanu et al., 2013] R. Pascanu, T. Mikolov, and Y. Bengio. On the difficulty of training recurrent neural networks. In *ICML*, pages 1310–1318, 2013.
- [Pascanu et al., 2014] R. Pascanu, C. Gulcehre, K. Cho, and Y. Bengio. How to construct deep recurrent neural networks. In *ICLR*, 2014.
- [Robinson and Fallside, 1987] A. J. Robinson and F. Fallside. The utility driven dynamic error propagation network. Technical Report CUED/F-INFENG/TR.1, Cambridge University, Engineering Department, 1987.
- [Schmidhuber, 2015] J. Schmidhuber. Deep learning in neural networks: An overview. *Neural Networks*, 61:85–117, 2015.
- [Sutskever et al., 2014] I. Sutskever, O. Vinyals, and Q. V. Le. Sequence to sequence learning with neural networks, 2014. arXiv:1409.3215.
- [Tallec and Ollivier, 2018] C. Tallec and Y. Ollivier. Can recurrent neural networks warp time? In *ICLR*, 2018.
- [Tatoeba, 2020] Tatoeba. <https://tatoeba.org>, 2020. Retrieved 2020-05-05.
- [Vaswani et al., 2017] A. Vaswani, N. Shazeer, N. Parmar, J. Uszkoreit, L. Jones, A. N. Gomez, L. Kaiser, and I. Polosukhin. Attention is all you need. In *NIPS*, 2017.
- [Wang et al., 2019] Z. Wang, Y. Ma, Z. Liu, and J. Tang. R-transformer: Recurrent neural network enhanced transformer, 2019. arXiv:1907.05572.
- [Werbos, 1988] P. J. Werbos. Generalization of backpropagation with application to a recurrent gas market model. *Neural Networks*, 1(4):339–356, 1988.
- [Wu et al., 2016] Y. Wu, M. Schuster, Z. Chen, Q.V. Le, V. Quoc, M. Norouzi, W. Macherey, M. Krikun, Y. Cao, and Q. Gao. Google’s neural machine translation system: Bridging the gap between human and machine translation, 2016. arXiv:1609.08144.
- [Zaremba et al., 2014] W. Zaremba, I. Sutskever, and O. Vinyals. Recurrent neural network regularization, 2014. arXiv:1409.2329.
- [Zilly et al., 2017] J. G. Zilly, R. K. Srivastava, J. Koutník, and J. Schmidhuber. Recurrent highway networks. In *ICML*, 2017.

A Comparison of DMU and GRU

In the notation applied in this paper operation of a GRU [Cho et al., 2014a] layer can be expressed as

$$\begin{aligned}
 r_t &= W_r x_t + U_r h_{t-1} + b_r \\
 \hat{h}_t &= W_h x_t + U_h (\sigma(r_t) \circ h_{t-1}) + b_h \\
 z_t &= W_z x_t + U_z h_{t-1} + b_z \\
 h_t &= h_{t-1} \circ \sigma(z_t) + f(\hat{h}_t) \circ (\mathbf{1} - \sigma(z_t))
 \end{aligned}$$

where $W_r, U_r, W_h, U_h, W_z, U_z$ and b_r, b_h, b_z are matrices and vectors of weights. The operation of DMU is presented in eqs. (1) and (2). In the most straightforward configuration, this network is a layer of linear units. Then

$$\begin{aligned}
 \hat{h}_t &= W_h x_t + U_h h_{t-1} + b_h \\
 z_t &= W_x x_t + U_x h_{t-1} + b_x \\
 h_t &= h_{t-1} \circ \sigma(z_t) + f(\hat{h}_t) \circ (\mathbf{1} - \sigma(z_t))
 \end{aligned} \tag{A.1}$$

Therefore, DMU is simpler in this basic configuration, thus having fewer weights per memory cell than a layer of GRUs, as it does not have the reset gate. In the general configuration, DMU can apply an arbitrary nonlinear transformation to its state, which GRU is unable to do.

LSTM [Hochreiter and Schmidhuber, 1997] and RHN [Zilly et al., 2017] are based on different, much more complex equations with even more weights. LSTM has twice more weights per memory cell than DMU has in the basic configuration.

B Experiments

B.1 Architectures

We present architectures for each problem in Table 4 and Table 5. Corresponding hyperparameters can be found in Table 4. The recurrent subnetwork is characterized by the number of units in subsequent layers. For example, a GRU subnetwork with two layers of 10 and 20 neurons will be briefly denoted by (10, 20). A DMU block with two FNN layers of 10 and 20 neurons will be denoted by (10, 20, 10) to account for the

layer of memory cells within the block. In the data-based problems, we evaluate each module at varying depths. In all cases, the compared architectures have matching numbers of trained parameters. Hyperparameters for the models were selected based on the random and grid searches and then fine-tuned manually. The metric used to evaluate the hyperparameters was calculated on the validation subset in each case.

B.2 Training

The data is split into training, validation, and testing set. On synthetic problems, training continues until the loss reaches a specified threshold (10^{-6}) on the validation set or the training budget is depleted. The error is then registered on the testing set and presented here. We follow a similar procedure for real-life problems, except the training process is stopped once the optimizer reaches the final epoch. All metrics are calculated using the model from the epoch with the best metric score on the validation set.

We run the experiment five times for each modern task/model/depth combination and aggregate the results. Standard result aggregation, such as averaging loss over time, would not be interpretable in the synthetic tasks since training is often unstable in these experiments. Therefore, the results for each synthetic problem are presented for multiple thresholds of the loss value. We plot the number of experiment runs that have reached the threshold in or before the specific epoch for each threshold. These thresholds allow us to assess how fast and how likely the module converges to a specific loss value. Thus, we can gain an insight into the quality of the module. The quicker the algorithm reaches a particular threshold, the better. Convergence to lower thresholds is also preferable.

Hyperparameters used for each experiment/neural module are presented in Table 6 and Table 7. We use ADAM optimizer to train all architectures.

B.3 Hardware

Our experiments have been performed on a PC equipped with AMD™Ryzen 1920X, 64GB RAM, 4xNVidia™RTX 2070 Super.

B.4 Testing strategy

To evaluate synthetic tasks, we run an experiment for each module 51 times and aggregate the results. On real-life data tasks, we aggregate results over five runs for each recurrent module. We report metrics obtained in the `best` runs. These runs are selected based solely on their performance on the test set. Therefore, in some cases, metrics reported in the `best` column for the training dataset are worse than those in the `mean` column.

B.5 Adding problem

In this problem, the network should output the sum of two randomly selected elements in the sequence of numbers. Specifically, the network is fed with two-dimensional vectors $[a, b]$, where a is randomly chosen from the interval $[-1, 1]$, and $b \in \{-1, 0, 1\}$ is a marker: -1 denotes the first and last element of the sequence, there are two pairs marked by 1, the rest are marked by 0. The task of the network is to output the

sum of a -s accompanied by b -s equal to 1 at the end of the sequence. Each network analyzed is composed of a recurrent block and a layer with softmax activation.

B.6 Temporal order

This task evaluates network’s ability to model temporal ordering of data. The input and the output are both 8-dimensional. They represent one of 8 symbols by one-hot encoding. The input symbols are: E (start), B (end), X or Y . X or Y occur at time t_1, t_2, t_3 . In all three of these occurrences the choice of X or Y is random, the rest of a sequence is filled with symbols a, b, c, d also selected at random. Sequence length is chosen randomly between 100 and 110. t_1, t_2, t_3 are selected randomly for each sequence, respectively between 10-20, 33-43 and 66-76. The output desired at the end of a sequence is either Q, R, S, U, V, A, B, C , depending on the combination of symbols that has occurred at times t_1, t_2 and t_3 . Each network analyzed is composed of a recurrent block and a layer with softmax activation.

B.7 NoiseSeq

Long time lag problems force networks to hold to the state for a long duration of time. To test the modules under such conditions, we use noisy sequences. The network is fed with symbols one-hot encoded in n -dimensional vectors. An input sequence is, with equal probability 0.5, either (x, a_1, \dots, a_{n-2}) or (y, a_1, \dots, a_{n-2}) , where $x, y, a_1, \dots, a_{n-1}$ are selected on random prior to an experiment. The task of the network is to output the first symbol in the input sequence when at $n - 1$ -st step. Each analyzed neural network is composed of a recurrent block and a layer with softmax activation.

B.8 PolyMusic

Inputs and outputs are 88-dimensional. They represent the binary encoding of possible piano-rolls at a current timestep (in MIDI note numbers, between 21 and 108 inclusive). Sequences vary in length. The task of the model is to predict the next time step in the sequence (i.e., output at time t is equal to input at time $t + 1$). The loss function is a negative log-likelihood averaged over all time steps in the dataset/batch. The neural network is composed of a recurrent block and a layer with the sigmoid activation.

B.9 NatLang

Inputs and outputs are single number representations of the most frequent words in English and special tokens such as “unknown” or “end of sequence”. Sequences include 100 words. The goal of the network is to predict another word within the current sequence. The loss function is perplexity (categorical cross-entropy exponent). See [Zaremba *et al.*, 2014] for details. The whole neural network comprises a recurrent block, followed by a 100-neurons dense layer and an output layer with the softmax activation. For this experiment, the input word embedding is set to a small size (64) on purpose to limit overfitting.

B.10 Machine Translation

We use tokens representing words, punctuation marks, *sentence start*, and *sentence end* in all languages. Each token is

experiment		RNN	LSTM	GRU	RHN	DMU
NoiseSeq	rc. blk ¹	(5, 5)	(2, 2)	(2, 3)	((3, 3))	((5, 4))
	weights no.	595	880	687	672	573
Adding	rc. blk ¹	(5, 5)	(2, 2)	(3, 2)	((4, 3))	((5, 5))
	weights no.	111	99	108	136	106
TempOrd	rc. blk ¹	(6, 6)	(2, 3)	(2, 4)	((4, 3))	((5, 6))
	weights no.	236	212	208	224	203

Table 4: Architectures used for the comparison of different neural modules in synthetic experiments.¹Recurrent block.

experiment	depth	RHN	DMU	weights no.
PolyMusic	1	100	100	46.7K
	2	100	122	66.9K
	5	100	131	127K
	10	100	136	228K
NatLang	1	100	100	1.7M
	2	100	122	1.7M
	5	100	131	1.8M
	10	100	136	1.9M
Translation	1	200	200	27.8M/36.6M/24.5M
	2	200	340	28.0M/36.8M/24.7M
	5	200	300	28.4M/37.3M/25.2M
	10	200	300	29.2M/38.1M/26.0M

Table 5: Architectures used for the comparison of RHN and DMU. We report the number of neurons in feedforward layers. The last layer of the DMU’s FNN on the Translation task always has 200 neurons. For the Translation task, weights’ numbers are provided for Spa2Eng, Ger2Eng, and Por2Eng, respectively.

encoded as a single, unique number. The goal is to translate Spanish/Portuguese/German sentences into English ones using a system with encoder-decoder architecture [Cho *et al.*, 2014b; Cho *et al.*, 2014a; Sutskever *et al.*, 2014]. A whole translator has encoder-decoder architecture. An encoder is a recurrent block. A decoder is composed of a recurrent block and a layer with the softmax activation. Additionally, we use input and output embeddings of size 650.

B.11 Learning rate ablation

Numerical results of this ablation are presented in Tables. 8–10. Note that this ablation does not make sense for the analyzed synthetic problems because the recurrent module is the entire architecture in these cases.

experiment	hyperparameter	RNN	LSTM	GRU	RHN	DMU
NoiseSeq	learning rate	0.01	0.002	0.05	0.05	0.02
	sequences per epoch	200	200	200	200	200
	min sequence length	100	100	100	100	100
	max epochs	100	100	100	100	100
Adding	learning rate	0.01	0.001	0.05	0.02	0.02
	sequences per epoch	200	200	200	200	200
	min sequence length	100	100	100	100	100
	max epochs	100	100	100	100	100
TempOrd	learning rate	0.01	0.005	0.02	0.02	0.05
	sequences per epoch	200	200	200	200	200
	min sequence length	100	100	100	100	100
	max epochs	100	100	100	100	100

Table 6: Hyperparameters used for synthetic tasks.

experiment	depth	hyperparameter	RHN	DMU
PolyMusic	all	max epochs	500	500
	1	learning rate	0.005	0.005
		weight decay	0.001	0.0001
		scheduler gamma	1.0	1.0
	2	learning rate	0.005	0.005
		weight decay	0.001	0.0001
		scheduler gamma	1.0	1.0
	5	learning rate	0.005	0.005
		weight decay	0.001	0.0001
		scheduler gamma	1.0	1.0
10	learning rate	0.005	0.002	
	weight decay	0.001	0.0001	
	scheduler gamma	1.0	1.0	
NatLang	all	max epochs	40	40
	1	learning rate	0.02	0.02
		weight decay	0.0001	0.0001
		scheduler gamma	0.9	0.9
	2	learning rate	0.02	0.02
		weight decay	0.0001	0.0001
		scheduler gamma	0.9	0.9
	5	learning rate	0.02	0.01
		weight decay	0.0001	0.0001
		scheduler gamma	0.9	0.98
10	learning rate	0.02	0.02	
	weight decay	0.0001	0.0001	
	scheduler gamma	0.9	0.98	
Spa2Eng/Por2Eng/Deu2Eng	all	teacher forcing ratio	1.0	1.0
	1	max epochs	50	50
		learning rate	0.01	0.005
		weight decay	0.0001	0.0001
	2	scheduler gamma	0.9	0.9
		learning rate	0.01	0.01
		weight decay	0.0001	0.0001
	5	scheduler gamma	0.9	0.9
		learning rate	0.01	0.003
		weight decay	0.0001	0.0001
10	scheduler gamma	0.9	1.0	
	learning rate	0.01	0.003	
	weight decay	0.0001	0.0001	
	scheduler gamma	0.9	1.0	

Table 7: Hyperparameters used for each experiment and each neural module.

depth	model	train			test		
		best	mean	std dev.	best	mean	std dev.
1	DMU-C	2.717	2.813	0.082	3.342	3.382	0.035
	DMU	2.942	2.959	0.042	3.567	3.631	0.050
2	DMU-C	2.991	3.034	0.197	3.430	3.486	0.041
	DMU	3.022	3.094	0.067	3.487	3.551	0.041
5	DMU-C	3.251	3.308	0.236	3.902	3.993	0.114
	DMU	3.215	3.208	0.064	3.630	3.685	0.032
10	DMU-C	3.752	nan	nan	4.262	5.032	0.632
	DMU	3.523	3.537	0.149	3.951	4.044	0.087

Table 8: PolyMusic: varied learning rate ablation results — loss. DMU-C stands for DMU with an equal learning rate for all modules.

depth	model	train			test		
		best	mean	std dev.	best	mean	std dev.
1	DMU-C	68.988	71.116	1.779	109.230	111.195	1.424
	DMU	56.625	59.422	3.137	105.354	106.129	0.475
2	DMU-C	81.311	81.014	1.691	117.555	118.166	0.647
	DMU	64.421	64.861	1.434	109.601	110.128	0.465
5	DMU-C	108.896	579.677	235.391	138.133	542.204	202.036
	DMU	92.395	94.063	1.114	117.924	120.368	1.456
10	DMU-C	696.302	697.572	0.688	642.178	642.914	0.436
	DMU	118.199	119.475	1.526	130.054	131.827	1.440

Table 9: NatLang: varied learning rate ablation results — perplexity. DMU-C stands for DMU with an equal learning rate for all modules.

lang pair	depth	model	train			test			
			best	mean	std dev.	best	mean	std dev.	
Spa2Eng	1	DMU-C	0.910	0.851	0.140	0.698	0.671	0.044	
		DMU	0.930	0.927	0.003	0.697	0.692	0.005	
	2	DMU-C	0.844	0.762	0.196	0.660	0.600	0.106	
		DMU	0.938	0.937	0.009	0.691	0.686	0.005	
	5	DMU-C	0.710	0.660	0.055	0.617	0.586	0.033	
		DMU	0.837	0.829	0.007	0.661	0.653	0.005	
	10	DMU-C	0.336	0.299	0.019	0.352	0.305	0.024	
		DMU	0.760	0.749	0.009	0.629	0.625	0.003	
	Por2Eng	1	DMU-C	0.941	0.929	0.019	0.777	0.771	0.005
			DMU	0.926	0.941	0.008	0.776	0.773	0.003
2		DMU-C	0.937	0.925	0.021	0.754	0.745	0.013	
		DMU	0.955	0.952	0.006	0.775	0.768	0.004	
5		DMU-C	0.766	0.625	0.203	0.699	0.590	0.164	
		DMU	0.861	0.861	0.004	0.731	0.725	0.005	
10		DMU-C	0.315	0.316	0.001	0.322	0.320	0.002	
		DMU	0.807	0.803	0.012	0.709	0.706	0.003	
Ger2Eng		1	DMU-C	0.923	0.915	0.017	0.749	0.748	0.001
			DMU	0.924	0.925	0.006	0.753	0.749	0.003
	2	DMU-C	0.884	0.898	0.009	0.730	0.722	0.005	
		DMU	0.935	0.938	0.005	0.749	0.743	0.004	
	5	DMU-C	0.724	0.702	0.019	0.662	0.647	0.014	
		DMU	0.845	0.843	0.010	0.711	0.703	0.006	
	10	DMU-C	0.443	0.336	0.055	0.446	0.344	0.053	
		DMU	0.797	0.782	0.011	0.684	0.679	0.004	

Table 10: Translation: varied learning rate ablation results — accuracy. DMU-C stands for DMU with an equal learning rate for all modules.